Cancer Letters 459 (2019) 50–58

Contents lists available at ScienceDirect

Cancer Letters

journal homepage: www.elsevier.com/locate/canlet

Original Articles

p53-dependent upregulation of miR-16-2 by sanguinarine induces cell cycle arrest and apoptosis in hepatocellular carcinoma

Beilei Zhang[a,b,1], Xinan Wang[a,1], Jiacong Deng[c], Haifeng Zheng[a], Wei Liu[d], Si Chen[a], Jie Tian[a,e,f,**], Fu Wang[a,*]

[a] Engineering Research Center of Molecular and Neuro Imaging, Ministry of Education, School of Life Science and Technology, Xidian University, Xi'an, Shaanxi, 710071, China
[b] Department of Gynecology and Obstetrics, Tangdu Hospital, The Fourth Military Medical University, Xi'an, Shaanxi, 710038, China
[c] School of Ocean Science and Biochemistry Engineering, Fujian Normal University Fuqing Branch, Fuqing, Fujian, 350300, China
[d] Department of Hepatobiliary Surgery, Xijing Hospital, The Fourth Military Medical University, Xi'an, Shaanxi, 710032, China
[e] CAS Key Laboratory of Molecular Imaging, Institute of Automation Chinese Academy of Sciences, Beijing, 100190, China
[f] Beijing Advanced Innovation Center for Big Data-Based Precision Medicine, School of Medicine, Beihang University, Beijing, 100190, China

ARTICLE INFO

Keywords:
miRNA-16
p53
Sanguinarine
Cell cycle
Apoptosis

ABSTRACT

MicroRNAs (miRNAs) were involved in cancer progression, and the targeting of miRNAs by natural agents has opened avenues for cancer treatment and drug development. miR-16 functions as a tumor suppressor and is frequently deleted or downregulated in various human cancers, including hepatocellular carcinoma (HCC). In the present study, we employed a miR-16-responsive luciferase reporter to screen candidate compounds that modulate miR-16 expression from a natural product library. One compound, sanguinarine (SG), was capable of activating miR-16 in HCC cells with wildtype or mutated p53 expression but not in p53-deleted HCC cells. Mechanistic investigations revealed that SG increased p53 occupancy on the miR-16-2 promoter and decreased the expression of miR-16 target genes, including Bcl-2 and cyclin D1. Moreover, SG significantly inhibited HCC cell proliferation in a p53-dependent manner by inducing cell cycle arrest and reactive oxygen species (ROS)-associated apoptosis. Silencing miR-16 by treatment with anti-miR16 miRNA inhibitors rescued the cell viability repression effect caused by SG. Importantly, SG dramatically suppressed tumor growth in an HCC xenograft model, with little cytotoxicity. Taken together, our results provide a preclinical proof-of-concept for SG as a potential strategy for HCC treatment based on the restoration of miR-16 tumor suppressor function.

1. Introduction

Hepatocellular carcinoma (HCC) is the leading cause of cancer-related deaths globally due to its low long-term survival rate and high recurrence rate within 10 years [1]. It is urgent and imperative to identify new targets and to develop effective therapeutics for HCC. Of note, microRNAs (miRNAs) are a class of small noncoding RNAs and have been shown to regulate multiple fundamental biological processes, including cell growth, the cell cycle, apoptosis and cancer progression [2,3]. Growing evidence indicates that miRNAs are dysregulated in various cancers and function as oncogenes or tumor suppressors [4]. For instance, miR-16 and miR-34a are frequently downregulated or deleted in various cancers, including human HCC [5–7]. These miRNAs induce cell cycle arrest and apoptosis and inhibit cellular proliferation by targeting a series of genes, such as cyclin D1, cyclin E or B-cell lymphoma (Bcl-2) [8–11]. In contrast, miR-21 is one of the first miRNAs found in human genome and is overexpressed in many different types of human cancers [12–14]. In addition, miR-21 upregulation is significantly associated with cancer progression and poor patient prognosis [15]. These studies indicate that deregulated miRNAs could be applied as potential biomarkers for cancer diagnosis and therapeutics.

Natural agents are an important source of valuable pharmaceutical reagents. More than 50% of the available drugs are indeed natural substances or their derivates. Numerous natural products exert a wide variety of cytotoxic effects against cancer cells via different mechanisms

* Corresponding author.
** Corresponding author. Engineering Research Center of Molecular and Neuro Imaging, Ministry of Education, School of Life Science and Technology, Xidian University, Xi'an, Shaanxi, 710071, China.
E-mail addresses: jie.tian@ia.ac.cn (J. Tian), fwang@xidian.edu.cn (F. Wang).
[1] These authors contributed equally to this work.

https://doi.org/10.1016/j.canlet.2019.05.042
Received 21 November 2018; Received in revised form 26 May 2019; Accepted 29 May 2019

[16]. Notably, several natural agents have been found to exert anti-tumor properties by altering the expression profiles of certain miRNAs [17]. For example, resveratrol, a polyphenolic phytoalexin abstracted from grape, was reported to inhibit glioma cell growth by down-regulating multiple miRNAs (miR-19, miR-21, miR-30a-5p) and upregulating the expression of their targets, which are crucial for glioma development [18]. Sophocarpine, one of the most abundant active ingredients in *Sophora alopecuroides* L, suppressed head and neck cancer progression and reversed epithelial-mesenchymal transition (EMT) by blocking miR-21 maturation [14]. Additionally, curcumin was shown to increase miR-203 expression and reduce the expression levels of its target genes, Akt2 and Src, ultimately triggering bladder cancer cell apoptosis and inhibiting proliferation [19]. All these studies support the idea that the specific targeting of miRNAs by natural agents could be a new avenue for cancer treatment.

In this study, we developed a luciferase reporter approach for screening natural agents from a natural product library with the ability to activate the tumor suppressor miRNA-16. By employing this reporter, the natural compound sanguinarine (SG) was identified to upregulate miR-16 expression in HCC cells. Furthermore, we demonstrated that SG was capable of suppressing tumor growth *in vitro* and in nude mouse model via inducing G0/G1 cell cycle arrest and apoptosis in a p53-dependent manner.

2. Materials and methods

2.1. Cell lines and reagents

All the HCC cell lines were purchased from Cell Bank of the Chinese Academy of Sciences and cultured in Dulbecco's Modified Eagle's medium (DMEM) supplemented with 10% fetal bovine serum (Gibco, CA) at 37 °C in 5% CO_2. The natural agent library containing 140 natural compounds was purchased from Selleck Chemicals (Houston, TX). siRNA targeting p53 (si-p53) were purchased from Shanghai GenePharma Co. The sequence of si-p53 is as follows: 5′- GCA UGA ACC GGA GGC CCA U dTdT-3’.

2.2. Plasmid construction

For the miR-16 screening reporter, the luciferase vector pGL3-control (Promega, WI) was digested with the *XbaI* restriction enzyme. DNA oligos containing three miR-16 binding sites were synthesized and annealed. Then, the annealed DNA oligos were ligated into the pGL3-control vector to obtain a miR-16 screening reporter. The sequences of the DNA oligos are as follows: miR-16 S: 5′-TAG CAG CAC GTA AAT ATT GGC GTA GCA GCA CGT AAA TAT TGG CGT AGC AGC ACG TAA ATA TTG GCG-3’; and miR-16 AS: 5′-CGC CAA TAT TTA CGT GCT GCT ACG CCA ATA TTT ACG TGC TGC TA C GCC AAT ATT TAC GTG CTG CTA-3’. For the full-length (FL) miR-16-1/miR16-2 or miR-16-2 fragment promoter reporter, PCR was performed to amplify the full-length miR-16-1/miR16-2 promoter or the corresponding fragment of the miR-16-2 promoter. Then, the PCR product was cloned into the pGL3-enhancer vector (Promega, WI). All the luciferase reporters were sequenced before use. The primers used for cloning the miR-16-1/miR16-2 FL or miR-16-2 fragment promoter were as follows: miR-16-1/FL: 5′-TTA AGA GAT TGA TAA ATG ATT TTT-3′, 5′-ATA CTC TAC AGT TGT GTT TTA A-3’; miR-16-2/FL: 5′-TAA GAT AAT AAC ATA TTT AAG TG-3′, 5′-AGT ATG TCA GTT CAT CCA AA-3’; Frag.1: 5′-AAG ATA ATA ACA TAT TTA AGT GG-3′, 5′-ACA AAA AGC ATA GAA TCA ATA ACA-3’; Frag.2: 5′-GTTTGGCTAT CGAGCACAAA-3′, 5′-AAC TAA TTC TAT GGA TTA AAA ACT-3’; and Frag.3: 5′-TCA GTA TGA AAT GAG TGA ATT T-3′, 5′-ATC TTG ACT GTA GCA TGT AAA-3’.

2.3. Compound screening with miR-16 reporter

HepG2 cells (5×10^3) were seeded into 96-well plates and incubated for 12 h at 37 °C in 5% CO_2. Then, HepG2 cells were co-transfected with miR-16 luciferase reporter and pRL-TK internal control plasmids. 24 h later, compounds from natural agent library (Selleck Chemicals, containing 140 natural compounds) were added to the cells at a final concentration of 10 μM. The complete medium with 0.1% DMSO was used as a control. After 24 h of incubation, the dual luciferase assay was performed.

2.4. Luciferase assay

The cells were cotransfected with the firefly luciferase reporter and an internal control plasmid, pRL-TK. At 24 h posttransfection, the cells were treated with SG (8 μM) for another 24 h. Then the cells were harvested and lysed. Luciferase activity was measured using a Dual Luciferase Reporter Assay Kit (Promega, WI) according to the manufacturer's protocols. The data presented were obtained from three independent experiments.

2.5. Real-time PCR

Total RNA from HCC cells with SG and/or siRNA treatment was extracted using the Trizol reagent (Invitrogen) according to the manufacturer's protocols. Reverse transcription and real-time PCR were performed as described previously [20]. Briefly, first-strand cDNA was obtained using a First-Strand cDNA Synthesis Kit (Invitrogen). Real-time PCR was performed using SYBR Green PCR Master Mix (Takara). The fold change of expression was calculated by the $2^{-\Delta\Delta Ct}$ method. U6 was used as an internal control for detecting miRNA expression. The sequences of the primers were as follows: miR-16-RT: 5′-GTC GTA TCC AGT GCG TGT CGT GGA GTC GGC AAT TGC ACT GGA TAC GAC CGC CAA T-3’; miR-16-F: 5′-TAG CAG CAC GTA AAT ATT GGC G-3’; miR-16-R: 5′-TGC GTG TCG TGG AGT C-3’; U6-F: 5′-GCT TCG GCA GCA CAT ATA CTA AAA T-3’; and U6-R: 5′-CGC TTC ACG AAT TTG CGT GTC AT-3’.

2.6. Western blotting

The protein (25 μg) from HCC cells with SG or siRNA treatment were separated by SDS-PAGE and transferred to PVDF membranes as described previously [21]. Primary antibodies (anti-Cyclin D1, anti-Bcl-2, anti-p53, Santa Cruz Biotechnology) were incubated with membranes at 4 °C overnight. After washing with TBST (Tris-buffered saline plus Tween-20) three times, the membranes were incubated with an IgG-HRP secondary antibody (anti-β-actin, Santa Cruz Biotechnology) for 1 h. Protein expression were determined using an ECL Western Blotting Detection Kit (GE Healthcare).

2.7. Cell viability assay

Cell viability was measured using a Cell Counting Kit-8 (CKK-8) assay (Beyotime Biotechnology, China) according to the manufacture's protocols. Briefly, 1×10^3 cells were seeded in 96-well plates and treated with different doses of the drug and/or miRNA inhibitors for 48 h. Then, 10 μl of CKK-8 was added to each well and incubated for 4 h. Absorbance at 450 nm was measured using a microplate reader (Synergy HT, Biotech).

2.8. Flow cytometry analysis

The cell cycle and apoptosis were analyzed using flow cytometry (BD Pharmingen, MI) as described previously [22]. For cell cycle analysis, the cells were harvested and washed with cold PBS and then suspended in 1 ml of propidium iodide (PI, Beyotime Biotechnology, China) solution containing 50 mg/ml PI, 100 mg/ml RNase A, and 0.1% (w/v) sodium citrate for 30 min. Flow cytometric analyses were performed to determine the relative DNA content in cells. For apoptosis

analysis, the harvested cells were suspended in 1 ml of annexin-V binding buffer containing 2.5 mM $CaCl_2$, 140 mM NaCl and 10 mM HEPES/NaOH. Then, FITC-conjugated annexin-V was added to the cell solution and incubated for 15 min, followed by the addition of PI (5 μg/ml). The apoptotic cells were measured by counting the annexin-V positive cells (right quadrant) using flow cytometry.

2.9. ROS measurement

ROS production was measured using an ROS assay kit (Beyotime Biotechnology, China) according to the manufacture's protocols. Briefly, the cells were treated with different doses (0, 0.5, 1, 2, 4 μM) of SG. Then, the cells were incubated with 10 mM DCFH-DA at 37 °C for 30 min. ROS production was assessed by measuring the optical density (OD) values at excitation/emission wavelengths of 488/525 nm.

2.10. In vitro caspase activity assay

Caspase activities were measured using caspase-3, -8, -9 activity kits (R&D Systems) according to the manufacture's protocols. Briefly, the cells were lysed, and the supernatants were collected by centrifugation at 12,000 rpm for 10 min. Then, the substrates Ac-DEVD-pNA for caspase-3, IETD-pNA for caspase-8, and LEHD-pNA for caspase-9 were added to each sample and incubated for 1 h at 37 °C. The optical density of each sample was quantified at a wavelength of 405 nm.

2.11. Immunohistochemical staining and TUNEL assay

The paraffin-embedded tissue sections were incubated with a primary antibody against Ki-67 (1:500 dilution, Santa Cruz Biotechnology) overnight at 4 °C, followed by incubation with a secondary antibody at 37 °C for 1 h. The mean number of positive cells were calculated from three random fields per slide. Terminal deoxynucleotidyl transferase–mediated dUTP nick-end labeling (TUNEL) staining was performed to analyze the apoptotic cells in tumor tissues using a TUNEL assay kit (Abcam) according to the manufacture's protocols. Images of the tumor sections were taken using a fluorescent microscope. The number of TUNEL-positive cells or Ki-67 positive cells were counted by averaging positive cells from three random fields per slide.

2.12. Chromatin immunoprecipitation assay

Chromatin immunoprecipitation (ChIP) assay was performed using an EZ ChIP Kit (Abcam) according to the manufacture's protocols. Briefly, 5×10^6 cells were crosslinked with 1% formaldehyde for 15 min. Crosslinked chromatin was sonicated and incubated overnight with IgG antibody or p53 antibody (Cell Signaling Technology). The immunoprecipitated DNA was purified and quantitated by real-time PCR to measure p53 binding levels, which were normalized to 2% input. The primers for ChIP assay were as follows: miR-16 promoter: 5′-TTC CAT GCT GTT TTG GTC CC-3′, 5′-ACC CAC CTC CAA ACA AGC CT-3'; P21 promoter: 5′-AAC ATG CTT GGG CAG CAG GC-3′, 5′-AGC CAC CAG CCT CTT CTA TGC CA-3′.

2.13. In vivo animal study

All animal experiments were approved by the Animal Experimental Ethics Committee of Xidian University. BALB/c nude mice (4 weeks old) were purchased from the Animal Center of Chinese Academy of Medical Science (Beijing, China). To establish a xenograft tumor model, 5×10^6 HepG2 cells were suspended in 100 μl of PBS and subcutaneously injected into the flanks of nude mice. When the tumors reached approximately 100 mm^3, the mice were randomly divided into two groups (n = 5) and intraperitoneally received SG (10 mg/kg) or saline every 2 days. Tumor volume was measured as [(length × width × height)/2]. After treatment for 21 days, the mice were sacrificed by cervical dislocation method, and tumor tissues were collected for immunohistochemical staining, TUNEL assay, Western blot and real-time PCR. For the cytotoxicity analysis, the blood from mice was harvested and used to measure alanine aminotransferase (ALT) and aspartate aminotransferase (AST) content using an ALT or AST activity assay kit (Abcam) according to the manufacture's protocols.

2.14. Statistical analysis

All data are expressed as mean ± SD from three separate experiments performed in triplicate. The differences between means were analyzed with Student's t-test. GraphPad Prism 5 (GraphPad Software, La Jolla, CA, USA) was used for statistical analysis. P values less than 0.05 were considered statistically significant.

3. Results

3.1. Identification of SG as a potent activator of miR-16

To screen the small-molecule modulators of miR-16, we first established a luciferase reporter that contained three complementary sequences of miR-16 in the 3' untranslated region (UTR) of the pGL3-control vector (Fig. 1A). Meanwhile, the pGL3-control empty vector containing no miR-16-binding sequence was used as a control. Theoretically, when the cells are transfected with this luciferase reporter and treated with natural agents, the natural agent would affect the expression of endogenous miR-16 and result in a change in luciferase activity. To verify this luciferase reporter, HepG2 cells were co-transfected with the luciferase reporter and an internal control luciferase plasmid, pRL-TK. Then, the cells were treated with different concentrations of miR-16 mimics. As shown in Fig. 1B, the luciferase signal decreased with an increasing dose of exogenous miR-16, suggesting that our luciferase reporter is responsive to the miR-16 level. Thus, we used this luciferase reporter to screen miR-16 modulators by measuring the luciferase signals in the following experiment.

The screening procedure is described in Fig. 1C. After a primary screening of 140 natural products in HepG2 cells (Supplementary Table S1), one hit compound named sanguinarine (SG) was identified as a potential miR-16 modulator. SG is a benzo-phenanthridine alkaloid and derived from the root of *Sanguinaria canadensis* and other poppy-fumaria species. We then reassayed the effect of SG on luciferase activity using the miR-16 reporter. As shown in Fig. 1D, the relative luciferase activity decreased in a dose-dependent manner. In contrast, SG resulted in no luciferase signal change in the pGL3 empty vector-transfected cells (Supplementary Fig. S1). These results indicate that SG inhibited luciferase activity of miR-16 reporter by regulating endogenous miR-16 expression.

3.2. SG upregulates miR-16 expression and downregulates its targets

To explore whether SG modulates miR-16 expression in HCC cells, three HCC cell lines (HepG2, Huh7 and Hep3B) were treated with SG, and then the expression of miR-16 both at the transcription level (primary miRs) and after their processing (mature miRs) was examined using real-time PCR analysis. As show in Fig. 2A, SG significantly increased mature miR-16 levels in HepG2 and Huh7 cells. However, SG had no effect on the expression of miR-16 in Hep3B cells. We then evaluated the efficacy of SG on the expression of primary miR-16. Similarly, we found that SG upregulated the primary miR-16 levels in both HepG2 and Huh7 cells but not in Hep3B cells (Fig. 2B). Notably, wildtype and mutant p53 were expressed in HepG2 and Huh7 cells, respectively, while p53 was deleted in Hep3B cells [23]. These results indicate that SG could upregulate miR-16 levels in HCC cells with wildtype or mutant p53 expression but not in HCC cells with p53 deletion.

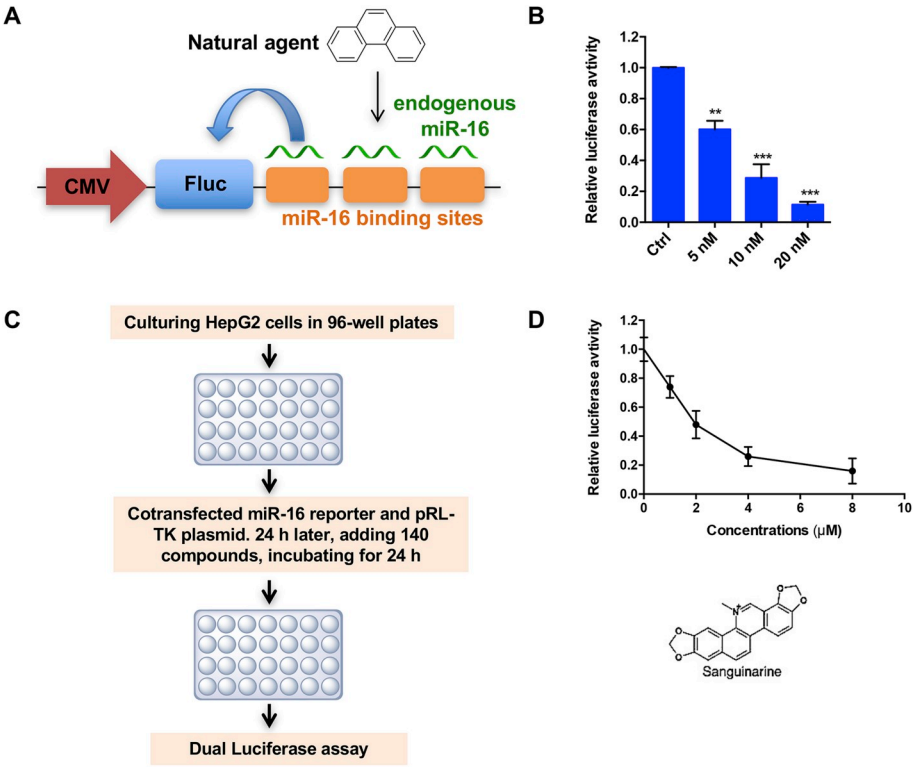

Fig. 1. Identification of miR-16 modulators through natural agent library screening. (A) Schematic illustration of the miR-16 luciferase reporter. Three complementary sequences of miR-16 were cloned into the 3′ UTR of the pGL3-control vector. After the natural agents are introduced into cells, they will affect endogenous miR-16 and result in luciferase activity change. (B) HepG2 cells were cotransfected with the miR-16 reporter and the luciferase plasmid pRL-TK, followed by treatment with different concentrations of miR-16 mimics. The relative luciferase activity was measured. (C) The screening procedure for the identification of miR-16 modulators. (D) HepG2 cells were transfected with the miR-16 luciferase reporter and pRL-TK and then treated with different concentrations of SG for 24 h. Cell lysates were subjected to a dual luciferase assay. Error bars represent the mean ± SD of three independent experiments. **p < 0.01, ***p < 0.001.

To exclude the possibility of nonspecific regulation on miR-16 expression by SG, we investigated the effects of SG on the other miRNAs that are related to HCC, including miR-21, miR-34a, miR-122 and miR-376a. The results showed that SG preferentially activated the expression of miR-16 but had no effect on other miRNAs in HepG2 cells (Supplementary Fig. S2). Next, we examined whether SG could regulate miR-16 functional targets. Several miR-16 target genes have been validated, such as cyclin D1 (CCND1) [8] and Bcl2 [24]. As demonstrated by the Western blot assay, the protein levels of CCND1 and Bcl-2 were remarkably reduced after SG treatment in HepG2 and Huh7 cells but not in Hep3B cells (Fig. 2C). Taken together, SG could upregulate miR-16 expression, thereby downregulating the levels of miR-16 targets.

3.3. SG activates miR-16-2 expression by increasing p53 occupancy on the miR-16-2 promoter

Since both mature and primary miR-16 levels were increased after SG treatment, we next examined whether SG could regulate miR-16 promoter activity. The mature products of miR-16 are known to be encoded by the *miR-16-1* and *miR-16-2* genes, which are located on chromosomes 13 and 3, respectively [25]. Thus, we cloned the full length (FL) miR-16-1 or miR-16-2 promoters into the 5' UTR of a luciferase gene (Fig. 3A). The three HCC cell lines (HepG2, Huh7 and Hep3B) were first transfected with the miR-16-1 FL or miR-16-2 FL luciferase reporter and then treated with SG. The luciferase activity of

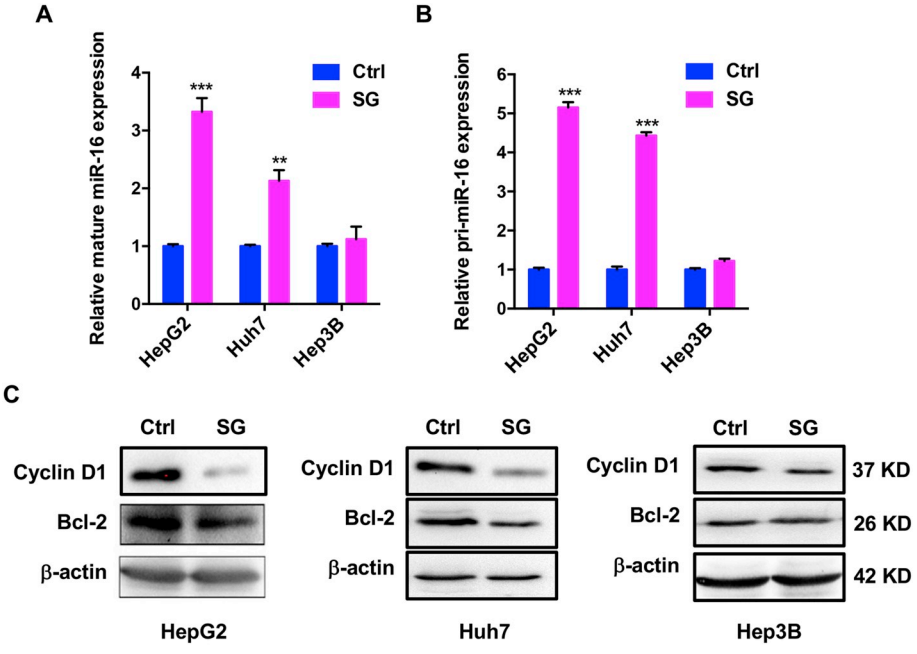

Fig. 2. SG increased miR-16 expression and decreased miR-16 targets in HCC cells. (A–B) HepG2, Huh7 and Hep3B cells were treated with 8 μM SG or vehicle control for 48 h. Then, total RNA was extracted and subjected to real-time PCR to measure the (A) mature miR-16 or (B) primary miR-16 expression level. (C) Western blot analysis of CCND1 and Bcl2 expression in cells treated as described in (A) and (B). Error bars represent the mean ± SD of three independent experiments. **p < 0.01, ***p < 0.001.

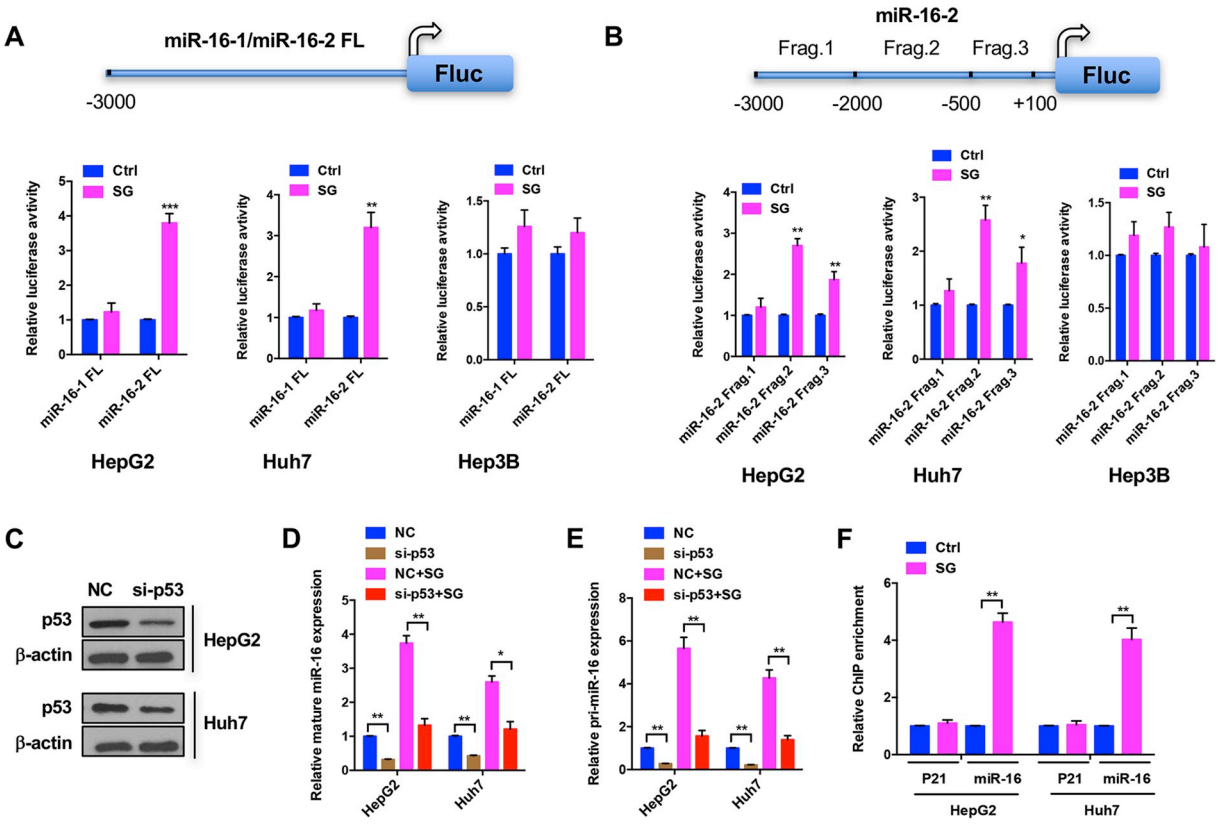

Fig. 3. SG increased p53 occupancy on the miR-16–2 promoter. (A) The upper panel shows a schematic of the promoter reporter containing the full-length miR-16-1 or miR-16-2 promoter sequences in the 5′UTR of the firefly luciferase (Fluc) gene. The miR-16-1 FL or miR-16-2 FL promoter reporter and the pRL-TK plasmid were cotransfected into HepG2, Huh7 and Hep3B cells. Dual luciferase activity was measured after treatment with 8 μM SG. (B) The upper panel shows a schematic of three fragments of the miR-16-2 promoter that were cloned into the 5′ UTR of the Fluc gene. The three fragments of the promoter reporters were transfected into HCC cells and assayed for luciferase activity as described above. (C) Western blot to detect the p53 protein expression in HepG2 or Huh7 cells after transfection with 100 nM siRNAs targeting p53 (si-p53). (D–F) HepG2 and Huh7 cells were treated with si-p53 (100 nM) and then treated with 8 μM SG. (D) The mature miR-16 or (E) primary miR-16 level was measured by real-time PCR. (F) A ChIP assay was performed in HepG2 and Huh7 cells treated with 8 μM SG. Real-time PCR was used to quantify p53 occupancy on the miR-16 and p21 promoter regions. Error bars represent the mean ± SD of three independent experiments. *$p < 0.05$, **$p < 0.01$.

the miR-16-2 FL promoter increased after SG treatment in HepG2 and Huh7 cells but not in Hep3B cells. In contrast, no luciferase activity change was observed in the miR-16-1 FL promoter reporter-transfected HCC cells. These results suggest a potential role for p53 in SG-regulated miR-16-2 promoter activity, and the miR-16-1 promoter was not dependent on the presence of p53.

To further examine which fragment of the miR-16-2 promoter responded to SG and p53, three fragments containing the 3000-bp upstream sequence of the miR-16-2 promoter were individually cloned and used for promoter activity assays. As shown in Fig. 3B, miR-16-2 Frag 2 and Frag 3 exhibited significantly increased luciferase signals in both HepG2 and Huh7 cells in the presence of SG but not in Hep3B cells. In contrast, the luciferase signal showed no obvious change in miR-16-2 Frag 1 reporter-transfected HCC cells after SG treatment. We then conducted Western blot experiments to examine the p53 expression and found that no significant change in p53 expression level after SG or miR-16 treatment in HepG2 and Huh7 cells (Supplementary Fig. S3). Subsequently, we employed an siRNA targeting p53 (si-p53) to knock down both wildtype and mutant p53 expression (Fig. 3C), followed by SG treatment in HepG2 and Huh7 cells. It was observed that mature miR-16 levels decreased after p53 knockdown (Fig. 3D). Moreover, the increased expression of miR-16 induced by SG was significantly attenuated by p53 knockdown. Analogously, primary miR-16 expression showed a similar change to that of mature miR-16 in HepG2 and Huh7 cells (Fig. 3E). To further determine whether p53 was directly bound to the promoter of the *miR-16-2* gene, a ChIP assay was performed using a p53-specific antibody. As shown in Fig. 3F, SG treatment significantly increased p53 occupancy on the miR-16 promoter in both HepG2 and Huh7 cells. In contrast, SG failed to raise p53 occupancy on the p21 promoter, which was reported to be a p53-binding region [26]. We then investigated the nuclear location of p53 after SG treatment. The confocal microscopy results revealed the increased nuclear localization of p53 after SG treatment for 24 h (Supplementary Fig. S4). Taken together, these results suggest that p53 directly bound to the promoter region of the *miR-16-2* gene and that SG increased p53 occupancy on the miR-16-2 promoter.

3.4. SG inhibits HCC cell proliferation and induces cell cycle arrest

We next examined the effect of SG on tumor cell biologic characteristics, especially proliferation and the cell cycle. Three HCC cell lines (HepG2, Huh7 and Hep3B) and one normal hepatic cell line, HL-7702, were treated with different concentrations of SG. Cell viability was then determined by the CKK-8 assay. As shown in Fig. 4A, SG significantly inhibited the proliferation of HepG2 and Huh7 cells in a dose-dependent manner. However, there was little growth repression in Hep3B or HL-7702 cells, suggesting that SG caused no cytotoxicity to HCC cells without p53 expression or normal human hepatocytes.

We then examined whether SG inhibited HCC cell proliferation through the regulation of miR-16 expression. HepG2, Huh7 and Hep3B cells were treated with miR-16 inhibitors (anti-miR16) and then treated with SG. As shown in Fig. 4B, SG treatment caused a significant inhibition of cell viability in HepG2 and Huh7 cells, while anti-miR16 attenuated the growth inhibitory effect of SG. In contrast, SG had no

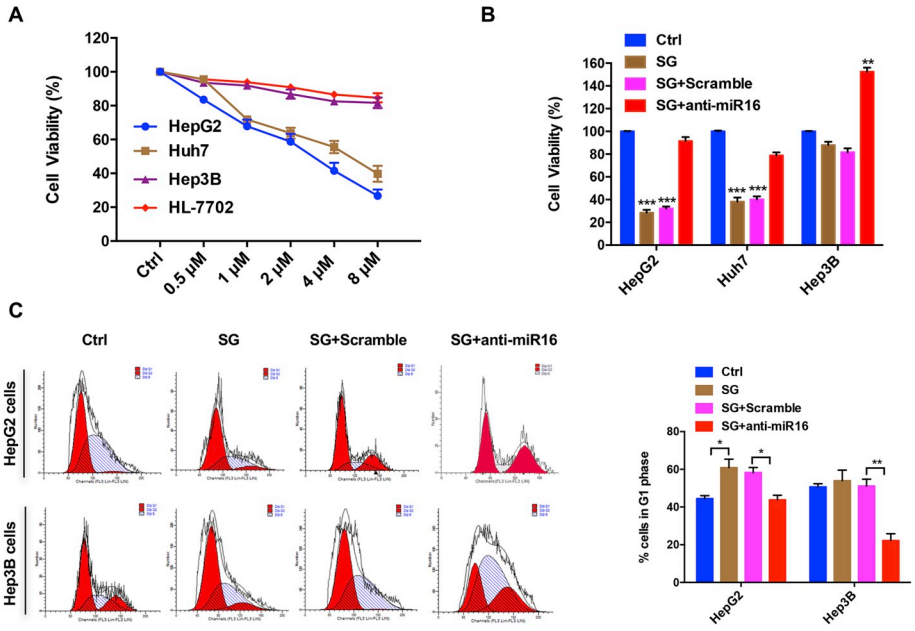

Fig. 4. SG inhibited HCC cell growth and induced cell cycle arrest. (A) HCC cell lines, HepG2, Huh7, Hep3B and HL-7702 cells were treated with different concentrations of SG for 48 h. Cell viability was measured by the CKK-8 assay. (B) HepG2, Huh7 and Hep3B cells were treated with SG at a concentration of 8 μM alone or in combination with 100 nM anti-miR16 inhibitors for 48 h. Cell viability was measured by the CKK-8 assay. (C) HepG2 and Hep3B cells were treated with SG alone or with anti-miR16 together as described in (B). Then, cell cycle distribution was analyzed using flow cytometry. Error bars represent the mean ± SD of three independent experiments. *p < 0.05, **p < 0.01, ***p < 0.001.

repression effect on Hep3B cell growth. Anti-miR16 and SG cotreatment promoted cell growth compared with SG and scramble RNA cotreatment in Hep3B cells, consistent with the fact that silencing miR-16 could stimulate cell viability. These results suggest that SG inhibited HCC cell growth by regulating miR-16 expression. We then asked whether SG induced cell cycle arrest through miR-16. Cell cycle analysis demonstrated that SG treatment resulted in a significant accumulation of cells in G0/G1 phase in HepG2 cells but had no influence on the cell cycle in Hep3B cells (Fig. 4C). However, anti-miR16 rescued the G1 cell cycle arrest caused by SG when the HepG2 cells were treated with SG and anti-miR16. The G1 population was markedly decreased in anti-miR16-treated Hep3B cells. Together, these results indicate that SG represses HCC cell proliferation and G1/S cell cycle transition by modulating miR-16 expression.

3.5. SG induced-apoptosis is associated with ROS production

To further reveal the mechanisms underlying the cell growth inhibitory effect of SG, a subsequent investigation on apoptosis was performed. HCC cells transfected with scramble RNA or anti-miR16 inhibitors were treated with SG or left untreated (Fig. 5A). Compared with the control group, treatment with SG alone induced an increase in annexin V-positive cells in HepG2 cells but not in Hep3B cells. Conversely, anti-miR16 significantly attenuated the population of apoptotic cells caused by SG in HepG2 cells. No obvious apoptotic cells were observed in Hep3B cells, suggesting that SG could induce apoptosis by modulating miR-16 in HCC cells with p53 expression. Since the induction of apoptosis may be related to the generation of intracellular reactive oxygen species (ROS), we then investigated whether SG could stimulate ROS production in HepG2 cells. As shown in Fig. 5B, the intracellular ROS release drastically increased with increasing concentrations of SG exposed to cells. To determine whether SG-induced ROS production was attributed to apoptosis induction, the cells were pretreated with a well-known ROS inhibitor, N-acetylcysteine (NAC), and coincubated with SG for another 24 h. The presence of NAC markedly prevented the SG-induced activation of caspases (caspase-3, -8 and -9) (Fig. 5C) and apoptotic cell death (Fig. 5D), as evidenced by the caspase activity assay and flow cytometer analysis. Collectively, these results indicate that SG-induced apoptosis is associated with ROS generation.

3.6. SG inhibits hepatocellular tumor growth in vivo

To determine the *in vivo* anti-tumor effect of SG, the HepG2 xenograft nude mice model was established, and tumor-bearing mice were intraperitoneally injected with SG (10 mg/kg) every 2 days. As shown in Fig. 6A, the tumors in the control group demonstrated fast and stable growth, while tumors in the SG treatment group exhibited marked growth retardation ($p < 0.01$). When comparing the tumor weights at the end of treatment, the average tumor weights from the SG group were significantly less than those from control tumors (Fig. 6B). The expression levels of miR-16, CCND1 and Bcl2 in the tumor tissues were also measured by real-time PCR (Fig. 6C) or Western blot analysis (Fig. 6D). In SG-treated tumors, the miR-16 levels were increased, while the expression of miR-16 targets CCND1 and Bcl2 was decreased, consistent with the *in vitro* results. Notably, no significant body weight loss was observed during the whole treatment process (Fig. 6E). Moreover, no obvious side effect was noted at the end of the experiment, as revealed by alanine aminotransferase (ALT) (Fig. 6F) and aspartate aminotransferase (AST) (Fig. 6G), which did not change before and after treatment. H&E staining results confirmed that SG does not cause any obvious organ toxicity (Supplementary Fig. S5). Immunohistochemistry (IHC) staining was further performed to assess the *in vivo* antiproliferative effect of SG (Fig. 6H). Qualitative analysis demonstrated a significant decrease in the average number of Ki-67-positive cells after SG treatment. In addition, TUNEL staining showed that the average number of apoptotic cells increased more than 3-fold in the SG-treated group compared with the control group (Fig. 6H). Taken together, these results suggest that SG represses HCC growth by inhibiting cell proliferation and triggering apoptosis, with no discernible toxicity. The underlying mechanism of SG on the inhibition of HCC cell growth through regulation miR-16-2 is depicted in Fig. 7.

4. Discussion

The dysregulation of cell cycle progression and apoptosis are hallmarks of numerous human cancers. Therefore, modulating cell cycle progression by small molecules has been considered a potent approach for cancer treatment. Our results demonstrated that SG was capable of inducing G1 phase cell cycle arrest and apoptosis in HCC cells with wildtype or mutant p53 expression. Moreover, we proved that SG could upregulate miR-16 expression and downregulate its target genes,

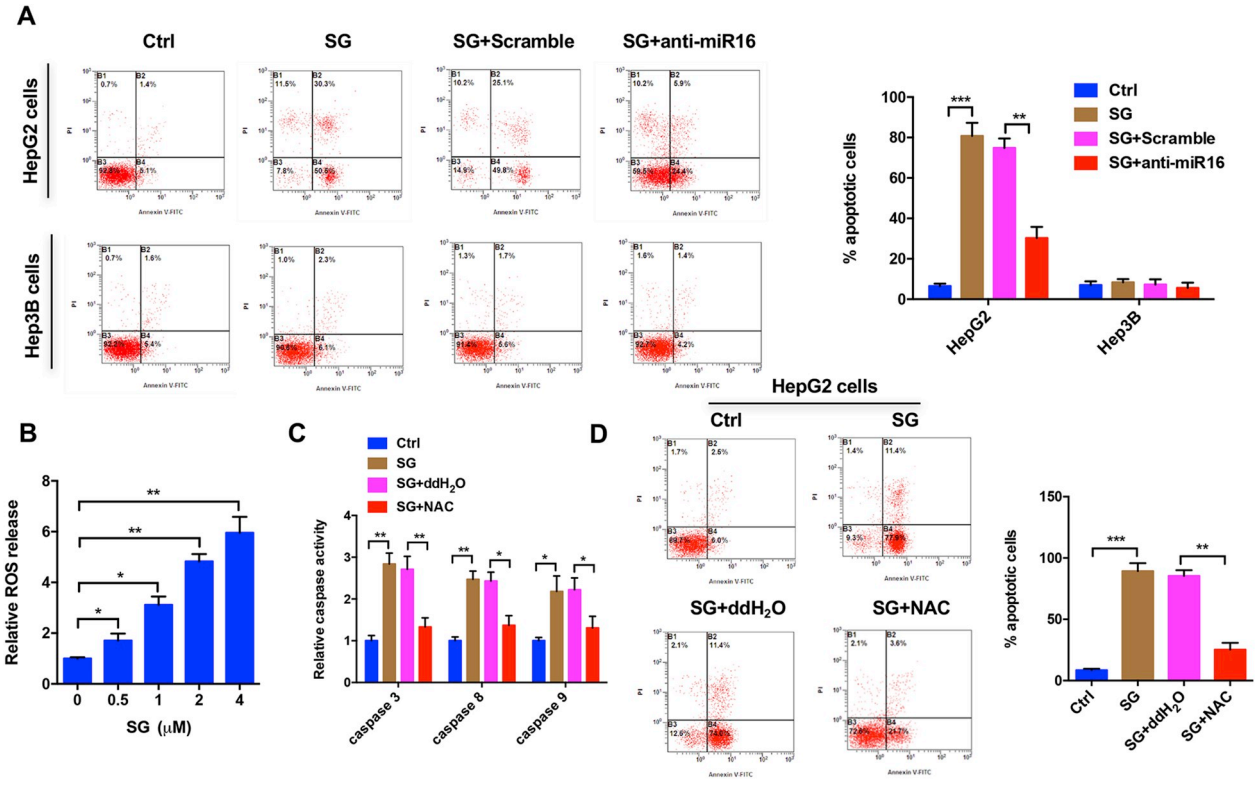

Fig. 5. SG-induced apoptosis is associated with ROS production. (A) HepG2 and Hep3B cells were treated with SG alone (8 μM) or in combination with anti-miR16 (100 nM) for 48 h. The cells were then collected and stained with FITC-conjugated annexin-V and PI for flow cytometry analysis. (B) HepG2 cells were treated with different concentrations of SG for 24 h and then incubated with 10 mM DCFH-DA at 37 °C for 30 min. ROS production was measured as the OD values. (C) HepG2 cells were treated with or without NAC (10 mM) for 1 h before treatment with SG (8 μM) for 24 h. Caspase activity was measured using a caspase-3, -8, -9 activity kit. (D) HepG2 cells were treated as described in (C). The cells were collected and stained with FITC-conjugated annexin-V and PI for flow cytometry analysis. Error bars represent the mean ± SD of three independent experiments. $^{**}p < 0.01$, $^{***}p < 0.001$.

CCND1 and Bcl2, which are related to G1/S cell cycle transition and cell apoptosis (Fig. 7). These results indicate that SG could be a new candidate miR-16 activator and used for HCC cancer therapy.

MiR-16 is located at 13q14.3 and found to be frequently deleted or downregulated in chronic lymphocytic leukemia (CLL) [24], which was the first experimental evidence that miRNAs were involved in tumorigenesis. Subsequent studies have shown that miR-16 is downregulated in other solid tumors, such as prostate cancer, breast cancer and HCC [27]. This phenomenon indicates that miR-16 functions as a tumor suppressor and that re-expression of miR-16 in tumors represents a potential approach to cancer therapy. Indeed, such potential has been addressed in a number of studies. The restoration of miR-16 resulted in a significant repression of the tumorigenicity of leukemic cells in a xenograft tumor model [28]. Moreover, ectopic expression of miR-16 inhibited cell proliferation and invasion and induced cell apoptosis in colorectal cancer cells [29]. Although miRNA-based therapeutics have attracted increasing attention, few approaches have been developed to target specific miRNAs and modulate their activities. Here, we developed a luciferase reporter system to screen miR-16 modulators from a natural product library and identified SG as a miR-16 regulator in HCC cells. We showed that SG caused G1 phase cell cycle arrest and apoptosis by upregulating miR-16 expression. Our data also showed that SG-induced apoptosis was associated with the ROS generation, and blocking the production of ROS by pre-treatment with NAC prevented the SG-induced cell apoptosis and caspases activation. Therefore, the discovery of SG as a miR-16 activator could improve the current HCC therapeutic strategies.

SG, a bioactive benzophenanthridine alkaloid, is predominantly extracted from plants, including *Sanguinaria canadensis*, *Chelidonium majus*, and *Argemone mexicana* [30]. SG has been shown to possess various biological functions, such as antifungal, antimicrobial and anti-inflammatory properties [31]. In addition, some studies have reported that SG inhibited the growth of various cancer cells by inducing cell cycle arrest and apoptotic cell death [32–34]. However, SG-regulated miRNA expression in HCC cells has rarely been reported. In this study, we found that SG was able to activate miR-16 expression and stimulate cell cycle arrest and apoptosis by modulating miR-16. In addition to SG, other natural products have been reported to alter the expression profile of miR-16 in cancer cells. Curcumin, an antioxidant natural compound found in turmeric, was shown to upregulate miR-15a and miR-16 expression and lead to an induction of apoptosis in MCF-7 breast cancer cells [35]. Moreover, epigallocatechin-3-gallate (EGCG), a polyphenol flavonoid extracted from natural green tea, induced apoptosis in HepG2 cells by upregulating the expression of miR-16. Enhanced miR-16 expression caused the inhibition of its target Bcl-2, followed by mitochondrial dysfunction, cytochrome *c* release, and subsequent apoptosis [36]. These findings indicate that the development of natural products targeting miR-16 and regulating their activities would be a promising strategy for cancer treatment, especially in cancers with miR-16 deletion or downregulation.

Our results demonstrated that SG modulates miR-16 expression in HCC cells in a p53-dependent manner. P53 is a critical transcription factor that controls various biological processes, including the cell cycle, apoptosis, senescence and autophagy [37]. In addition, p53 is considered a tumor suppressor gene and is mutated or deleted in more than 50% of human cancers [38]. Our data showed that the activation of miR-16 expression by SG required wildtype or mutant p53, suggesting that mutant p53 could also regulate miR-16 expression. Our results also indicated that the function of mutant p53 could be regulated. In Huh7 cells with mutant p53 expression, the function of p53 is

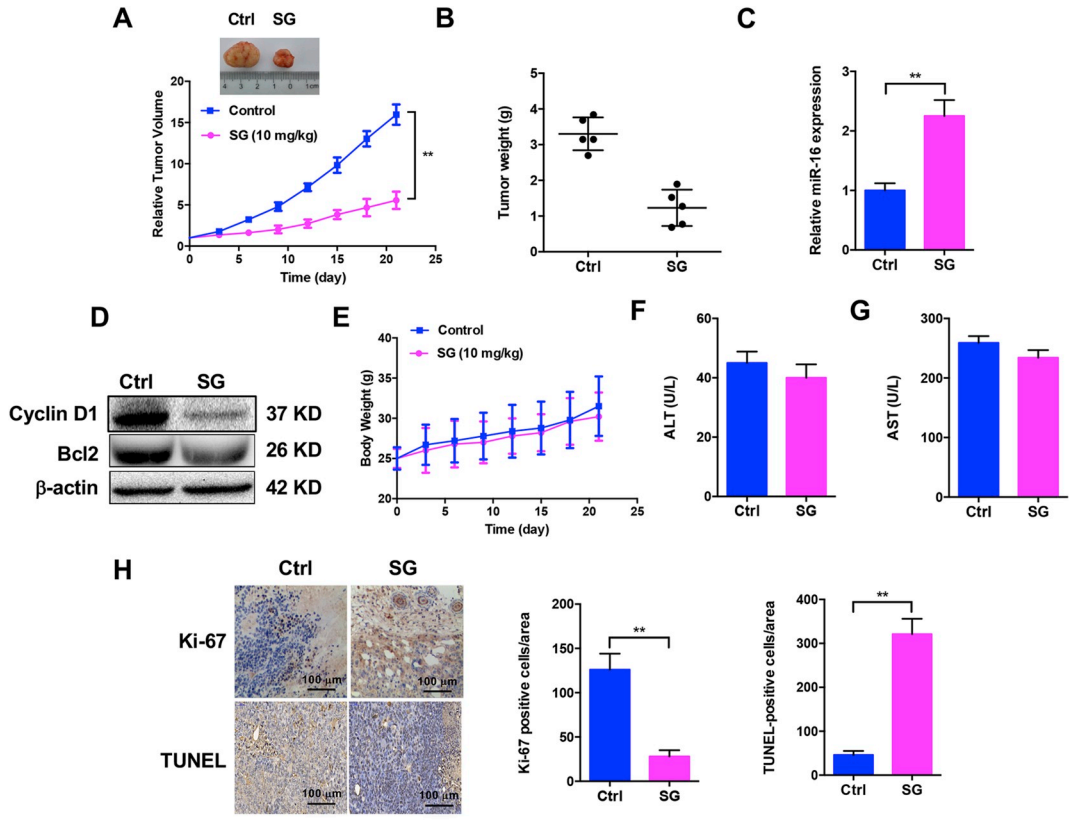

Fig. 6. Antitumor efficacy of SG examined in HepG2 xenograft tumor models. Tumor-bearing xenografted mice were intraperitoneally treated with SG (10 mg/kg) or saline every two days for three weeks. (A) Tumor volume and (B) tumor weight were measured during treatment. (C) The miR-16 expression level and (D) CCND1 and Bcl2 protein expression were determined in the tumor tissues using real-time PCR assay or Western blot. (E) Mouse body weights were monitored during the whole treatment process. (F and G) ALT and AST content was analyzed from mouse blood. (H) IHC and TUNEL staining were performed to determine Ki-67 expression and apoptotic cells in tumor samples. Error bars represent mean ± SD of three independent experiments. **p < 0.01.

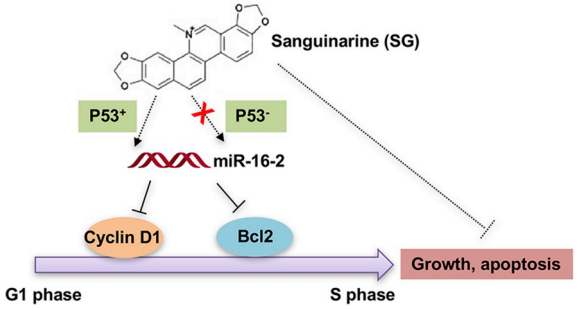

Fig. 7. Schematic model of HCC cell growth inhibition by SG in a p53-dependent manner. In HCC cells with wildtype or mutated p53 expression, SG upregulates miR-16-2 expression, resulting in the downregulation of CCND1 and Bcl-2 targets, inducing G1/S cell cycle arrest and apoptosis, and finally leads to cell growth inhibition. In p53-deleted HCC cells, cell growth inhibition does not occur.

diminished but not abrogated. It is likely that SG acts as a regulator to affect a specific molecular domain of p53, such as the transactivation domain or the DNA-binding domain, which is either in a suboptimal state in mutant p53 or in a normal state in wildtype p53. In this regard, it is understandable that SG did not activate miR-16 expression in Hep3B cells with p53 deletion. Our results also demonstrated that p53 bound to the promoters of *miR-16-2* gene but not *miR-16-1* gene, indicating that p53 transactivated miR-16 via binding to a specific region of the miR-16-2 promoter.

In conclusion, we identified a natural agent, SG, that could activate miR-16 expression in HCC cells with wildtype or mutant p53 but not p53-deleted cells. More importantly, SG was capable of suppressing tumor cell growth by inducing cell cycle arrest and apoptotic cell death. Therefore, SG could be a promising compound for treating HCC that harbors p53 in cancer cells.

Conflicts of interest

The authors declare no potential conflicts of interest.

Acknowledgements

This work was supported by the National Natural Science Foundation of China (Grant No. 81772010, 81571721) and the National Key Research and Development Program of China (973 Program) (Grant No. 2017YFA0205202).

Appendix A. Supplementary data

Supplementary data to this article can be found online at https://doi.org/10.1016/j.canlet.2019.05.042.

References

[1] J. Zheng, D. Kuk, M. Gonen, V.P. Balachandran, T.P. Kingham, P.J. Allen, M.I. D'Angelica, W.R. Jarnagin, R.P. DeMatteo, Actual 10-year survivors after resection of hepatocellular carcinoma, Ann. Surg. Oncol. 24 (2017) 1358–1366.
[2] I. Bentwich, A. Avniel, Y. Karov, R. Aharonov, S. Gilad, O. Barad, A. Barzilai, P. Einat, U. Einav, E. Meiri, E. Sharon, Y. Spector, Z. Bentwich, Identification of hundreds of conserved and nonconserved human microRNAs, Nat. Genet. 37 (2005) 766–770.
[3] J. Winter, S. Jung, S. Keller, R.I. Gregory, S. Diederichs, Many roads to maturity: microRNA biogenesis pathways and their regulation, Nat. Cell Biol. 11 (2009) 228–234.

[4] J.L. Mott, MicroRNAs involved in tumor suppressor and oncogene pathways: implications for hepatobiliary neoplasia, Hepatology 50 (2009) 630–637.
[5] A.A. Mohamed, Z.A. Ali-Eldin, T.A. Elbedewy, M. El-Serafy, F.A. Ali-Eldin, H. AbdelAziz, MicroRNAs and clinical implications in hepatocellular carcinoma, World J. Hepatol. 9 (2017) 1001–1007.
[6] Y. Dang, D. Luo, M. Rong, G. Chen, Underexpression of miR-34a in hepatocellular carcinoma and its contribution towards enhancement of proliferating inhibitory effects of agents targeting c-MET, PLoS One 8 (2013) e61054.
[7] N.E. El-Abd, N.A. Fawzy, S.M. El-Sheikh, M.E. Soliman, Circulating miRNA-122, miRNA-199a, and miRNA-16 as biomarkers for early detection of hepatocellular carcinoma in Egyptian patients with chronic hepatitis C virus infection, Mol. Diagn. Ther. 19 (2015) 213–220.
[8] Q. Liu, H. Fu, F. Sun, H. Zhang, Y. Tie, J. Zhu, R. Xing, Z. Sun, X. Zheng, miR-16 family induces cell cycle arrest by regulating multiple cell cycle genes, Nucleic Acids Res. 36 (2008) 5391–5404.
[9] A.L. Kasinski, F.J. Slack, miRNA-34 prevents cancer initiation and progression in a therapeutically resistant K-ras and p53-induced mouse model of lung adenocarcinoma, Cancer Res. 72 (2012) 5576–5587.
[10] F. Wang, X.D. Fu, Y. Zhou, Y. Zhang, Down-regulation of the cyclin E1 oncogene expression by microRNA-16-1 induces cell cycle arrest in human cancer cells, BMB Rep 42 (2009) 725–730.
[11] C. Welch, Y. Chen, R.L. Stallings, MicroRNA-34a functions as a potential tumor suppressor by inducing apoptosis in neuroblastoma cells, Oncogene 26 (2007) 5017–5022.
[12] R. Kumarswamy, I. Volkmann, T. Thum, Regulation and function of miRNA-21 in health and disease, RNA Biol. 8 (2011) 706–713.
[13] F. Wang, B. Zhang, L. Zhou, Y. Shi, Z. Li, Y. Xia, J. Tian, Imaging dendrimer-grafted graphene oxide mediated anti-mir-21 delivery with an activatable luciferase reporter, ACS Appl. Mater. Interfaces 8 (2016) 9014–9021.
[14] W. Liu, B. Zhang, G. Chen, W. Wu, L. Zhou, Y. Shi, Q. Zeng, Y. Li, Y. Sun, X. Deng, F. Wang, Targeting mir-21 with sophocarpine inhibits tumor progression and reverses epithelial-mesenchymal transition in head and neck cancer, Mol. Ther. 25 (2017) 2129–2139.
[15] L.X. Yan, X.F. Huang, Q. Shao, M.Y. Huang, L. Deng, Q.L. Wu, Y.X. Zeng, J.Y. Shao, MicroRNA miR-21 overexpression in human breast cancer is associated with advanced clinical stage, lymph node metastasis and patient poor prognosis, RNA 14 (2008) 2348–2360.
[16] S. Nobili, D. Lippi, E. Witort, M. Donnini, L. Bausi, E. Mini, S. Capaccioli, Natural compounds for cancer treatment and prevention, Pharmacol. Res. 59 (2009) 365–378.
[17] Y. Li, D. Kong, Z. Wang, F.H. Sarkar, Regulation of microRNAs by natural agents: an emerging field in chemoprevention and chemotherapy research, Pharm. Res. (N. Y.) 27 (2010) 1027–1041.
[18] G. Wang, F. Dai, K. Yu, Z. Jia, A. Zhang, Q. Huang, C. Kang, H. Jiang, P. Pu, Resveratrol inhibits glioma cell growth via targeting oncogenic microRNAs and multiple signaling pathways, Int. J. Oncol. 46 (2015) 1739–1747.
[19] S. Saini, S. Arora, S. Majid, V. Shahryari, Y. Chen, G. Deng, S. Yamamura, K. Ueno, R. Dahiya, Curcumin modulates microRNA-203-mediated regulation of the Src-Akt axis in bladder cancer, Cancer Prev. Res. 4 (2011) 1698–1709.
[20] F. Wang, X. Song, X. Li, J. Xin, S. Wang, W. Yang, J. Wang, K. Wu, X. Chen, J. Liang, J. Tian, F. Cao, Noninvasive visualization of microRNA-16 in the chemoresistance of gastric cancer using a dual reporter gene imaging system, PLoS One 8 (2013) e61792.
[21] G. Chen, J. Chen, Y. Qiao, Y. Shi, W. Liu, Q. Zeng, H. Xie, X. Shi, Y. Sun, X. Liu, T. Li, L. Zhou, J. Wan, T. Xie, H. Wang, F. Wang, ZNF830 mediates cancer chemoresistance through promoting homologous-recombination repair, Nucleic Acids Res. 46 (2018) 1266–1279.
[22] F. Wang, Z. Wang, N. Hida, D.O. Kiesewetter, Y. Ma, K. Yang, P. Rong, J. Liang, J. Tian, G. Niu, X. Chen, A cyclic HSV1-TK reporter for real-time PET imaging of apoptosis, Proc. Natl. Acad. Sci. U. S. A. 111 (2014) 5165–5170.
[23] S.P. Hussain, J. Schwank, F. Staib, X.W. Wang, C.C. Harris, TP53 mutations and hepatocellular carcinoma: insights into the etiology and pathogenesis of liver cancer, Oncogene 26 (2007) 2166–2176.
[24] A. Cimmino, G.A. Calin, M. Fabbri, M.V. Iorio, M. Ferracin, M. Shimizu, S.E. Wojcik, R.I. Aqeilan, S. Zupo, M. Dono, L. Rassenti, H. Alder, S. Volinia, C.G. Liu, T.J. Kipps, M. Negrini, C.M. Croce, miR-15 and miR-16 induce apoptosis by targeting BCL2, Proc. Natl. Acad. Sci. U. S. A. 102 (2005) 13944–13949.
[25] L. Lezina, N. Purmessur, A.V. Antonov, T. Ivanova, E. Karpova, K. Krishan, M. Ivan, V. Aksenova, D. Tentler, A.V. Garabadgiu, G. Melino, N.A. Barlev, miR-16 and miR-26a target checkpoint kinases Wee1 and Chk1 in response to p53 activation by genotoxic stress, Cell Death Dis. 4 (2013) e953.
[26] O. Laptenko, R. Beckerman, E. Freulich, C. Prives, p53 binding to nucleosomes within the p21 promoter in vivo leads to nucleosome loss and transcriptional activation, Proc. Natl. Acad. Sci. U. S. A. 108 (2011) 10385–10390.
[27] R.I. Aqeilan, G.A. Calin, C.M. Croce, miR-15a and miR-16-1 in cancer: discovery, function and future perspectives, Cell Death Differ. 17 (2010) 215–220.
[28] G.A. Calin, A. Cimmino, M. Fabbri, M. Ferracin, S.E. Wojcik, M. Shimizu, C. Taccioli, N. Zanesi, R. Garzon, R.I. Aqeilan, H. Alder, S. Volinia, L. Rassenti, X. Liu, C.G. Liu, T.J. Kipps, M. Negrini, C.M. Croce, MiR-15a and miR-16-1 cluster functions in human leukemia, Proc. Natl. Acad. Sci. U. S. A. 105 (2008) 5166–5171.
[29] C. You, H. Liang, W. Sun, J. Li, Y. Liu, Q. Fan, H. Zhang, X. Yue, J. Li, X. Chen, Y. Ba, Deregulation of the miR-16-KRAS axis promotes colorectal cancer, Sci. Rep. 6 (2016) 37459.
[30] H. Ahsan, S. Reagan-Shaw, J. Breur, N. Ahmad, Sanguinarine induces apoptosis of human pancreatic carcinoma AsPC-1 and BxPC-3 cells via modulations in Bcl-2 family proteins, Cancer Lett. 249 (2007) 198–208.
[31] J. Lenfeld, M. Kroutil, E. Marsalek, J. Slavik, V. Preininger, V. Simanek, Antiinflammatory activity of quaternary benzophenanthridine alkaloids from Chelidonium majus, Planta Med. 43 (1981) 161–165.
[32] C. Fu, G. Guan, H. Wang, The anticancer effect of sanguinarine: a review, Curr. Pharmaceut. Des. 24 (2018) 2760–2764.
[33] Y. Wang, B. Zhang, W. Liu, Y. Dai, Y. Shi, Q. Zeng, F. Wang, Noninvasive bioluminescence imaging of the dynamics of sanguinarine induced apoptosis via activation of reactive oxygen species, Oncotarget 7 (2016) 22355–22367.
[34] V.M. Adhami, M.H. Aziz, S.R. Reagan-Shaw, M. Nihal, H. Mukhtar, N. Ahmad, Sanguinarine causes cell cycle blockade and apoptosis of human prostate carcinoma cells via modulation of cyclin kinase inhibitor-cyclin-cyclin-dependent kinase machinery, Mol. Cancer Ther. 3 (2004) 933–940.
[35] J. Yang, Y. Cao, J. Sun, Y. Zhang, Curcumin reduces the expression of Bcl-2 by upregulating miR-15a and miR-16 in MCF-7 cells, Med. Oncol. 27 (2010) 1114–1118.
[36] W.P. Tsang, T.T. Kwok, Epigallocatechin gallate up-regulation of miR-16 and induction of apoptosis in human cancer cells, J. Nutr. Biochem. 21 (2010) 140–146.
[37] R. Beckerman, C. Prives, Transcriptional regulation by p53, Cold Spring Harb Perspect Biol 2 (2010) a000935.
[38] A.J. Levine, p53, the cellular gatekeeper for growth and division, Cell 88 (1997) 323–331.